ANNALS of Clinical and Translational Neurology
Open Access
ANA American Neurological Association since 1875

BRIEF COMMUNICATION

Unusual Stüve-Wiedemann syndrome with complete maternal chromosome 5 isodisomy

Mariarosa A. B. Melone[1], Michael J. Pellegrino[2], Maria Nolano[3], Beth A. Habecker[2], Stefan Johansson[4,5], Neil M. Nathanson[6], Per M. Knappskog[4,5], Angelika F. Hahn[7] & Helge Boman[4,5]

[1]Division of Neurology and InterUniversity Center for Research in Neuroscience, Department of Clinical and Experimental Medicine and Surgery, Second University of Naples, Naples, Italy
[2]Department of Physiology and Pharmacology, OHSU School of Medicine, Portland, Oregon
[3]Neurology Division, 'Salvatore Maugeri' Foundation IRCCS, Medical Center of Telese Terme, Telese Terme, Benevento, Italy
[4]Department of Clinical Science, University of Bergen, Bergen, Norway
[5]Center of Medical Genetics and Molecular Medicine, Haukeland University Hospital, Bergen, Norway
[6]Department of Pharmacology, University of Washington, Seattle, Washington
[7]Department of Clinical Neurological Sciences, London Health Sciences Centre, Western University, London, Ontario, Canada

Correspondence
Helge Boman, Center for Medical Genetics and Molecular Medicine, Haukeland University Hospital, N-5021 Bergen, Norway.
Tel: (+47) 55975475; Fax: (+47) 55975479;
E-mail: helge.boman@helse-bergen.no

Funding Information
The study was supported in part through National Institutes of Health grant HL068231 to Professor Dr. Beth Habecker, PhD.

Received: 19 June 2014; Revised: 26 August 2014; Accepted: 27 August 2014

Annals of Clinical and Translational Neurology **2014; 1(11): 926–932**

doi: 10.1002/acn3.126

The core clinical data were presented in abstract form at the joint Congress of the Italian Association of Neuropathology and the Italian Association for Research on Brain Aging. Genova, Italy, 19–21 May 2011.

Abstract

A woman was isozygous for a novel mutation in the leukemia inhibitory factor receptor gene (*LIFR*) (c.2170C>G; p.Pro724Ala) which disrupts LIFR downstream signaling and results in Stüve-Wiedemann syndrome (STWS). She inherited two identical chromosomes 5 from her mother, heterozygous for the *LIFR* mutation. The presentation was typical for STWS, except there was no long bone dysplasia. Prominent cold-induced sweating and heat intolerance lead to an initial diagnosis of cold-induced sweating syndrome, excluded by exome sequencing. Skin biopsies provide the first human evidence of failed postnatal cholinergic differentiation of sympathetic neurons innervating sweat glands in cold-induced sweating, and of a neuropathy.

Introduction

Stüve-Wiedemann syndrome (STWS, MIM 601559), a severe autosomal recessive disorder, is due to mutations in the leukemia inhibitory factor receptor gene (*LIFR*) on chromosome 5p13.[1] Skeletal dysplasia, camptodactyly, severe sucking/swallowing difficulties, episodes of respiratory distress, and hyperthermia are manifest from birth and often result in early death. The few survivors to adolescence develop progressive scoliosis, joint contractures, and thermoregulatory difficulties akin to cold-induced sweating syndrome (CISS).[2,3] Complete maternal chromosome 5 isodisomy is only reported once.[4] We describe in a 33-year-old woman a fully manifest STWS without long bone dysplasia, caused by an isozygous *LIFR* mutation.

Subject and Methods

Blood was sampled from the patient, parents, and two siblings. Electrophysiological studies (median, ulnar, peroneal, sural nerves) followed standard techniques. Quantitative sensory testing (QST): Cold, warm, cold- and heat

pain thresholds were tested (foot, hand, thigh, and leg) using a thermal sensory analyzer (Medoc, Ramat Yishai, Israel) and methods of limits. Tactile thresholds and mechanical pain perception were evaluated using 18 calibrated Semmes–Weinstein monofilaments, and a calibrated monofilament with a bending force of 95 mN, connected to a probe. Sudomotor function was assessed by sympathetic skin responses (SSRs),[5] thermoregulatory sweat test (TST)[6] and dynamic sweat test (DST).[7] Autonomic cardiovascular reflexes were studied as described.[2]

Skin biopsy

Three millimeter punch biopsies were performed on four body sites: upper arm (hyperhidrotic area) and thigh, leg, and fingertip (anhidrotic areas). Samples were processed using indirect immunofluorescence technique, according to previously published procedures.[8] Primary antibodies (ABs) against protein gene product (PGP) 9.5 (pan-neuronal marker), myelin basic protein (MBP) (myelinated fibers), dopamine beta hydroxylase (DβH) (noradrenergic fibers), and vasoactive intestinal peptide (VIP) (cholinergic fibers) were used to visualize nerve fiber populations. ABs against Collagen IV (Col IV) and an endothelium-binding agglutinin (Ulex europaeus; UEA-1) were used to visualize Meissner corpuscle (MC) capsules and sweat glands (Col IV) and blood vessels (UEA-1). Quantification of epidermal nerve fibers (ENFs), intrapapillary myelinated endings (IMEs) and MCs was performed as previously described.[9] Both monoclonal mouse and polyclonal rabbit ABs were used in indirect immunofluorescence studies (see Table 1).

DNA analysis

First, single gene sequencing of cytokine receptor-like factor 1 (*CRLF1*), cardiotrophin-like factor 1 (*CLCF1*), interleukin 6 signal transducer (*IL6ST*) and *LIFR* was carried out. Then genome-wide single-nucleotide polymorphism (SNP) genotyping was performed with the Genome-Wide Human SNP array 6.0 (Affymetrix, Santa Clara, CA) and analyzed using PLINK v1.07.[10] Whole-exome sequencing was performed at Hudson Alpha Institute for Biotechnology (Huntsville, AL) using Roche-NimbleGen Sequence Capture EZ Exome v2 kit and paired-end 100nt sequencing on the Illumina HiSeq.[11] The reads were analyzed with Casava v.1.8 (Illumina , San Diego, CA) and aligned to hg19 reference genome using Burrows-Wheeler Alignment tool.[12] The chemical analysis was performed at Hudson Alpha Institute for Biotechnology. The chromosome 5 aligned sequence data resulted in 137X mean coverage of the target capture regions with more than 98% of target bases covered at least 8X. Cytogenetic studies were performed with blood lymphocytes and fibroblasts from four skin biopsies.

Cell culture and transfection, immunoblotting, and glycosylation

Hep3B2.1-7 cells, which do not express LIFR, were obtained from and cultured as recommended by American Type Culture Center (Manassas, VA). Cells were transfected with 1.5 μg DNA per well using Lipofectamine™ 2000 (Invitrogen, Carlsbad, CA) and transfection efficiency was assessed by GFP expression. Immunoblotting of cell lysates was carried out using antibodies against STAT3, tyrosine-phosphorylated STAT3 (Tyr705) (Cell Signaling Technology, Danvers, MA) and LIFR (C-19; Santa Cruz Biotechnology Inc, Santa Cruz, CA). Species-specific secondary antibodies conjugated to horseradish peroxidase (Pierce, Rockford, IL) were used to visualize bands with chemiluminescence.

Ethics

The research was performed according to the guidelines of the Declaration of Helsinki. All participating subjects provided informed consent.

Results

Clinical observations

Term delivery was uneventful (birth weight 2300 g). From birth she had severe difficulties swallowing and feeding,

Table 1. Name, target, source, and dilution of primary antibodies.

Antigen (abbreviation)	Target	Manufacturer	Dilution
Rabbit protein gene product 9.5 (rPGP)	Pan-neuronal marker	Biogenesis (Poole, UK)	1:400
Mouse protein gene product 9.5 (mPGP)	Pan-neuronal marker	AbD Serotec (Kidlington, UK)	1:800
Rabbit vasoactive intestinal peptide (rVIP)	Cholinergic nerve fibers	Immunostar (Hudson WI, US)	1:1000
Mouse vasoactive intestinal peptide (mVIP)	Cholinergic nerve fibers	Santa Cruz Biotechnology (Heidelberg, Germany)	1:300
Mouse collagen IV (mCOLIV)	Basement membrane and vessels	Chemicon (Billerica, MA, USA)	1:800
Mouse myelin basic protein (mMBP)	Myelinated nerve fibers	Santa Cruz Biotechnology (Heidelberg, Germany)	1:800
Rabbit dopamine beta hydroxylase (rDβH)	Noradrenergic nerve fibers	Chemicon (Billerica, MA, USA)	1:1000

which caused developmental and growth delay. During the first 2 years she suffered bouts of respiratory distress, pneumonia, and unexplained high fevers. She was noted to sweat very little in hot weather since age four, and still becomes easily overheated. Paradoxically, she sweats profusely on the face, arms, and upper trunk when exposed to cold temperatures or when stressed. At 18 months, she underwent talipes equino-varus correction and Achilles tendon lengthening. At 12 years, a severe and rapidly progressive thoracolumbar scoliosis was treated with spinal instrumentation. Despite early surgical intervention, she developed a moderate spastic paraparesis, diagnosed as spondylogenic cervical myelopathy.

Cognitive function and intellect were normal. She displayed typical dysmorphic features: narrow face, high arched palate, mild lower facial weakness and horizontal smile, low set ears, short stature, cubitus valgus and flexion contractures at the elbows, small hands with clinodactyly, thoracolumbar scoliosis and lumbar lordosis, a deformed left foot and misshaped toes. A plantar trophic ulcer required repeat debridement. At age 24, a mild axonal sensory-motor neuropathy was confirmed by electrophysiological studies. She remains ambulatory and leads a fairly normal life. Paradoxical sweating is adequately controlled with oral clonidine 0.1 mg twice daily and amitriptyline 10 mg once daily. She is now married and pregnant.

Investigations

Blood work was normal including hematologic parameters; blood sugar; liver, renal, and thyroid function; plasma-luteinizing and follicular-stimulating hormone, testosterone; resting plasma adrenaline, noradrenaline, dopamine, renin, and vasopressin. A skeletal survey was normal, aside from congenitally contracted elbow and ankle joints, and a severe rotatory thoracolumbar scoliosis. There was no bowing of long bones, nor internal cortical thickening, osteopenia, or signs of previous fractures (Fig. 1A and B). Although she had no sensory complaints, QST indicated distal sensory impairment for touch, warm, cold, noxious heat and cold pain, and mechanical pain evoked by pinprick. Electrophysiological studies were consistent with a length-dependent axonal neuropathy.

Autonomic assessment

Autonomic assessment demonstrated selective impairment of sudomotor function. TST revealed no sweat responses on raising her core temperature 1°C. In contrast, she sweated profusely on her face, neck, shoulders, arms, and upper trunk with ambient temperatures of 22°C or less, while fingers and the lower body remained dry. DST demonstrated in areas of hyperhidrosis (forearm) a pattern of pilocarpine-induced sweating that was similar to that induced by cold ambient temperatures with regard to sweat gland density and sweat volume (Fig. 1C). In areas of anhidrosis (leg) few sweat glands became activated by pilocarpine and with low sweat output (Fig. 1D). SSRs were of low amplitude on recording from the palm and were not recordable from the sole (data not shown).

Morphology of autonomic and sensory innervation of skin

Immunohistochemical studies of skin biopsies from hyperhidrotic and anhidrotic regions revealed an unusual pattern of autonomic and somatic cutaneous innervation (Fig. 1E–P). Areas of hyperhidrosis (upper arm) showed preserved epidermal and dermal innervation including sudomotor nerves, yet there was an abnormal expression of noradrenergic (DβH-ir) sudomotor fibers in place of the normal rich cholinergic (VIP-ir) innervation (Fig. 1G, K, and O). Biopsies from anhidrotic hairy and glabrous skin (the leg and fingertip, respectively) revealed severe cutaneous denervation with loss of sensory receptors and unmyelinated and myelinated somatic nerve fibers (Fig. 1H compared to G, and E compared to F, respectively and indicated by arrows), and with abnormalities of the surviving nerves, in particular the shortening of internodal lengths (Fig. 1I compared to J). In the anhidrotic hairy skin of the leg there was also evidence of autonomic denervation involving all skin adnexa – sweat glands (Fig. 1L compared to K), arteriovenous anastomoses (Fig. 1M compared to N), and piloerector muscles (Fig. 1P compared to O) – with a complete absence of cholinergic (VIP-ir) nerves (Fig. 1L, M, and P) and with few residual noradrenergic (DβH-ir) fibers (Fig. 1L and P). Together, the findings indicate a severe, possibly developmental derangement of somatic and autonomic innervation, with the most striking feature being the persistence of noradrenergic sudomotor fibers in the hyperhidrotic skin (indicated by arrows in Fig. 1K), which suggests a failed switch in noradrenergic to cholinergic phenotype. Developmental derangement may also have affected cutaneous nerve survival in most of the lower body.

Genetic testing revealed complete maternal isodisomy for chromosome 5 and a novel LIFR variant

The patient's karyotype was 46,XX. DNA sequencing identified homozygosity for a novel missense variant c.2170C>G in *LIFR* (Fig. S1) on 5p13 (NM_002310.5),

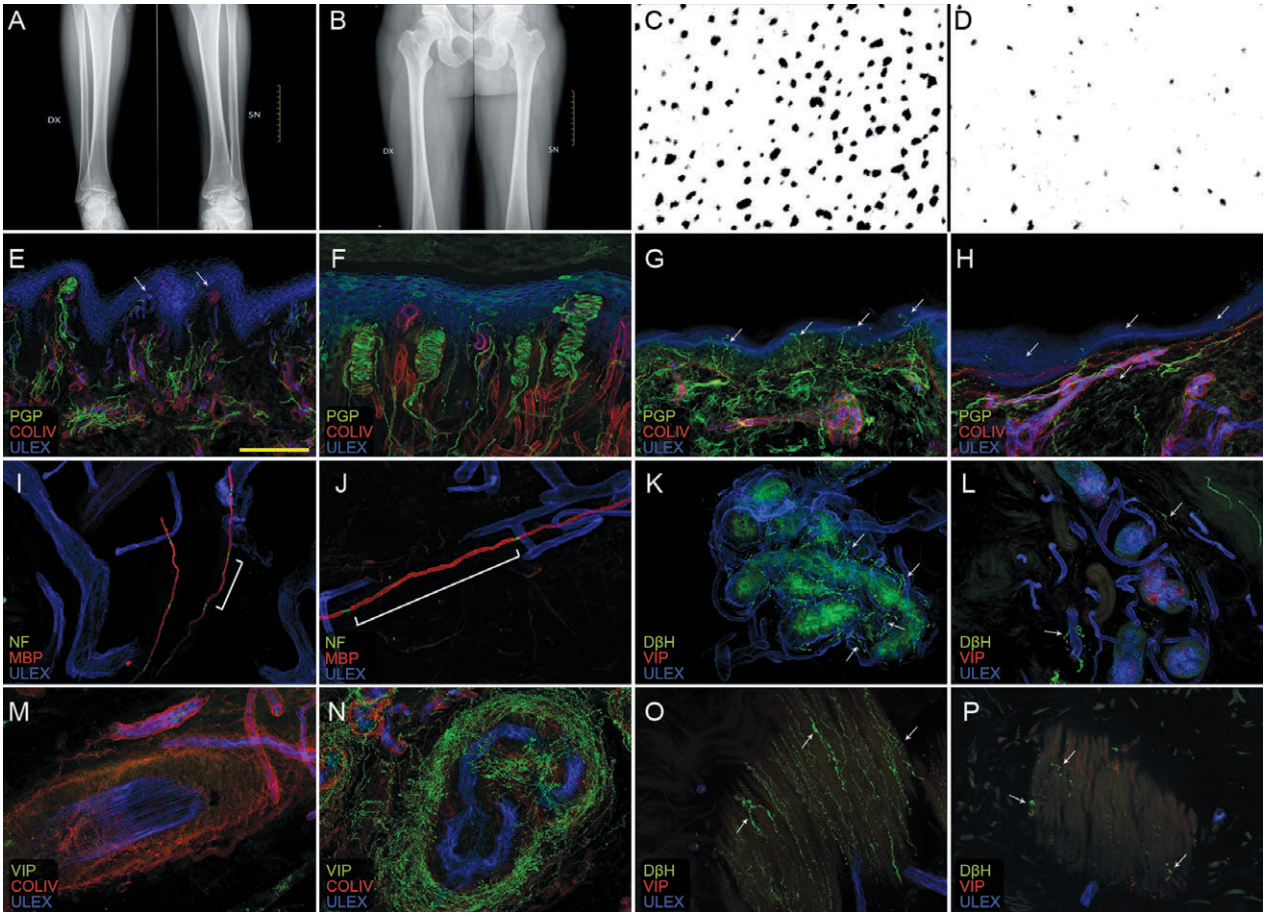

Figure 1. Radiographs, taken at age 32 years, of both the tibia and fibula (A) and of the femurs (B) show neither bowing, nor cortical thickening, or osteopenia. Evaluation of sweating by dynamic sweat test (DST) was carried out on the forearm (hyperhidrotic area, C) and the lower leg (anhidrotic area, D). The sweat imprints of the forearm illustrate a high density of sweat glands (123/cm^2; 5% cut-off 100/cm^2) with high sweat output (7.6 nL/min per gland; 5% cut-off 5.4 nL/min per gland) (C), while in the anhidrotic skin of the leg few sweat glands (15/cm^2; 5% cut-off 64/cm^2) became activated by pilocarpine and with low sweat output (3.0 nL/min per gland; 5% cut-off 5.6 nL/min per gland) (D). The cutaneous innervation of hairy and glabrous skin is illustrated in triple–immunostained confocal images (E–P). The skin biopsy from the upper arm (hyperhidrotic area; G, K, and O) shows a relatively preserved epidermal innervation (G, arrows) (19.0 ENF/mm; 5% cut-off 20.2 ENF/mm), but an abnormal expression of noradrenergic (DβH-ir) sudomotor fibers (K, highlighted by arrows) in place of the usually rich cholinergic (VIP-ir) innervation of sweat glands (note the complete absence of VIP staining); piloerector muscles present a normal noradrenergic innervation (O, arrows) but lack cholinergic fibers (absence of VIP staining). In the anhidrotic skin from the leg (H, L, and P) there is a severe epidermal (6.3 ENF/mm; 5% cut-off 12.7 ENF/mm) and dermal denervation (H, indicated by arrows) with lack of the normal cholinergic nerves and show only few scattered noradrenergic fibers around sweat glands (L, arrows) and along piloerector muscles (P, arrows). In the glabrous skin from the fingertip (E, I, M, control F, J, N), Meissner corpuscles are almost absent (E, arrows) (2.7 MC/mm^2, 5% cut-off 21.2 MC/mm^2) and there is a severe epidermal and dermal denervation, with the subepidermal neural plexus being completely deranged (compare E to F). The few myelinated fibers present in the patient's dermis have shortened internodes (58.1 $\pm$ 16.5 μm vs. 79.1 $\pm$ 13.8 μm) and are thinner than normal (compare I to J). There is a complete loss of cholinergic (VIP-ir) fibers in arteriovenous anastomoses (compare M to N). PGP, protein gene product 9.5; MBP, myelin basic protein; DβH, dopamine beta hydroxylase; VIP, vasoactive intestinal peptide; NF, pan-neurofascin; COLIV, collagen IV; ULEX, endothelium binding agglutinin; ENF, epidermal nerve fiber. Scale bar = 100 μm in E–H, K–N; 50 μm in I, J, O, P.

predicted to result in altered protein p.Pro724Ala. Genome-wide SNP arrays, including parental samples, revealed a complete maternal isodisomy for chromosome 5 with one crossing-over (Fig. 2). Mother carried the Pro724Ala variant in heterozygosity. No trace of paternal chromosome 5 was found in blood or cultured fibroblasts derived from four skin biopsies. Whole-exome sequencing confirmed the subject's isozygosity for the *LIFR* variant and ten rare variants (Table S1). DNA analysis revealed no sequence variants in *CRLF1*, *CLCF1*, IL6ST (encoding gp130), *OSMR* (encoding oncostatin M receptor), and *FAM134B*.

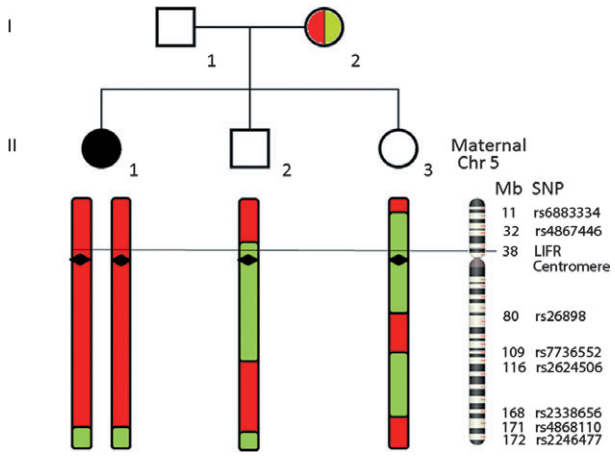

Figure 2. This figure illustrates uniparental isodisomy (UPD) chromosome 5. The patient (black symbol) is shown to have two completely identical chromosomes 5 from the mother by Affymetrix Genome-Wide Human single-nucleotide polymorphism (SNP) array 6.0. The three siblings have the same SNPs at the start of the chromosome. The SNP where the crossing-over occurred is given on the far right. The patient has only one crossing-over. The leukemia inhibitory factor receptor (*LIFR*) mutation (c.2170C>G; p.Pro724Ala) is indicated. The paternal contribution to the two siblings is omitted.

The LIFR p.Pro724Ala mutation alters LIFR function and glycosylation

Transfection of wild-type (WT) LIFR into Hep3B cells generated LIFR protein of three different molecular weights, while cells transfected with the Pro724Ala mutant ($LIFR^{P724A}$) contained only the smaller two forms of LIFR (Fig. 3A, asterisks). Glycosidase treatment with PNGaseF caused a downward shift in the higher molecular weight forms of both the WT and LIFR mutant to similar sizes (Fig. 3B), demonstrating that receptor glycosylation was altered in the Pro724Ala mutant. To determine if the mutant altered LIFR function, cells were treated with leukemia inhibitory factor (LIF) to stimulate downstream STAT3 phosphorylation. LIF stimulated robust STAT3 phosphorylation in WT LIFR-transfected cells (Fig. 3C), but little STAT3 phosphorylation in $LIFR^{P724A}$ transfected cells. The presence of STAT3 (Fig. 3C) and LIFR (Fig. 3D) protein was confirmed by western blot.

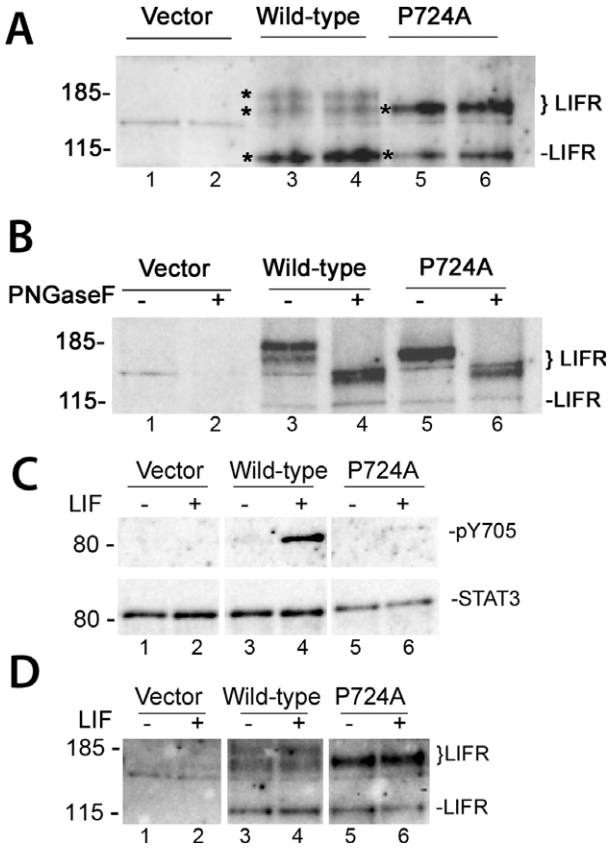

Figure 3. Leukemia inhibitory factor receptor (LIFR) P724A mutant has altered glycosylation and impaired signaling. LIFR-negative Hep3B cells were transfected in duplicate with pcDNA3 (Vector, lanes 1–2), wild-type LIFR (wild-type, lanes 3–4), or the LIFR mutant (P724A, lanes 5–6), and blotted for LIFR. Molecular weight standards are marked on the left (kD). (A) Asterisks denote LIFR bands. The P724A mutant lacks the highest molecular weight band. (B) Cell lysates were combined with 5% SDS, 0.4 M DTT and denatured at 100°C for 10 min prior to incubation with 0.5 M sodium phosphate, pH 7.5, 1% NP40, and with (+) or without (−) PNGaseF (Peptide -N-Glycosidase F) for 1 hr at 37°C to remove glycosylation, and blotted for LIFR. Wild-type and P724A-transfected cells had LIFR of similar size after PNGaseF treatment, suggesting altered glycosylation of P724A-mutant receptor. (C) Transfected cells were treated with LIF to stimulate downstream signaling through LIFR-gp130 complex. Cells expressing wild-type LIFR exhibited strong STAT3 phosphorylation (Y705), but cells expressing vector alone or the P724A mutant did not. Total STAT3 (STAT3) was readily detectable in all cells. (D) LIFR protein was abundant in P724A transfected cells, despite the lack of STAT3 phosphorylation. All blots are representative of at least three independent experiments.

Discussion

STWS was diagnosed in a 33-year-old female, isozygous for a *LIFR* mutation (c.2170C>G, p.Pro724Ala) and the entire chromosome 5. DNA analysis ruled out mutations in *CRLF1* and *CLCF1*, which can yield a similar neonatal phenotype associated with high mortality in infancy or early childhood.[3,13] Few STWS patients survive to adolescence and none has been reported pregnant.[3,14] Thus, our patient is exceptional.

She presented most neonatal STWS characteristics, yet lacked the congenital dysplasia of long bones, considered a hallmark of STWS.[1,3] Radiographs, taken in adulthood,

were normal, aside from congenital contractures at the elbows and ankles and a severe, partially corrected thoracolumbar scoliosis. Spinal deformities are reported in STWS long-term survivors and are invariably seen in juvenile CISS patients.[14,15] The two conditions also exhibit cold-induced hyperhidrosis on the face and upper body, and heat-induced hypohidrosis restricted to the lower body.[2,3] Paradoxical sweating and heat intolerance was observed starting at age four. The early symptom onset would be most consistent with a developmental anomaly of autonomic sudomotor function, a postulate supported by abnormal sweat gland innervation. Biopsies from areas of cold-induced hyperhidrosis showed relatively preserved epidermal and dermal sensory innervation, yet sweat glands lacked the normally rich cholinergic innervation[8] and retained instead an ample supply of noradrenergic sympathetic fibers. This was also true for other sympathetically innervated dermal adnexa – arteriovenous anastomoses and piloerector muscles. Similar findings had been documented in a CISS patient with compound heterozygocity of two *CRLF1* mutations.[16] These observations provide the first human evidence of a failed switch of adrenergic to cholinergic sympathetic innervation of sweat glands, causing paradoxical sweating. The LIFR mutant does not stimulate STAT3 phosphorylation. Impaired signaling through the CNTF/LIFR/gp130 tripartite complex accounts for the absence of cholinergic differentiation in sympathetic neurons innervating sweat glands.[17,18]

Skin biopsies from the leg showed a length-dependent dermal sensory and autonomic denervation. In the anhidrotic skin of the leg, few residual sweat glands were surrounded by scattered noradrenergic nerve fibers and ENF counts were reduced. Moreover, biopsies of glabrous skin from the fingertip, revealed denervation of the epidermis and dermis, including loss of MC's and their afferent myelinated fibers. These morphological findings correlate with the reduced tactile and nociceptive perception detected on QST. Abnormal sensation has not yet been documented in STWS and our patient had not voiced sensory complaints. A few clinical reports hinted at possible insensitivity to pain in CISS and STWS, as some children show little pain with recurring fractures.[13,19] These observations require future study. Given the complete chromosome 5 isodisomy, we considered and excluded, among others, the association of STWS and recessive sensory and autonomic neuropathy type 2 (HSAN II).[20]

The absence of long bone dysplasia remains unexplained, but may relate to the mutation.[21] The *LIFR* variant (c.2170C>G; p.Pro724Ala) is located to the first amino acid in the third fibronectin III motif, the proline being conserved throughout evolution. Our in vitro studies clearly indicate that the *LIFR* mutation alters the gene product and disturbs LIFR function. Thus, there is little doubt that the mutation is deleterious, causing STWS. Genome-wide SNP arrays revealed complete maternal isodisomy for chromosome 5. Cytogenetic studies yielded no paternal chromosome 5 material in blood cells or fibroblasts; cells were exclusively maternal. Thus, we conclude that the patient was the product of a paternal nullisomic rescue or, less likely, of an initial trisomy with subsequent loss of the paternal contribution.[22] This case exemplifies uniparental isodisomy as a possible, albeit rare, cause of autosomal recessive disorders.

Acknowledgments

The authors gratefully acknowledge the contribution of the following participating investigators: Francesca Califano, M.D. and Carla Schettino, M.D. who provided and cared for the study patient; Vincenzo Provitera, M.D. and Giuseppe Caporaso BS who participated in the autonomic testing and the morphological studies. Sigrid Erdal, Trude Høysæter, and Jorunn S. Bringsli provided expert technical assistance. Cell transfection experiments and functional studies of the LIFR mutant were supported by the National Institutes of Health grant HL068231 to Professor Beth Habecker, Ph.D.

Author Contributions

All authors contributed equally to the conception and execution of the various aspects of the work and to the study as a whole. They collectively vouch for the accuracy and integrity of the data. Dr. H. Boman assumed the leadership role in coordinating the contributions from three areas of expertise: Drs. M. A. B. Melone, M. Nolano, and A. F. Hahn were involved in the acquisition and interpretation of the clinical and neuropathological data. Drs. H. Boman, S. Johansson, and P. M. Knappskog directed the acquisition, analysis, and interpretation of the genetic data. Drs. M. J. Pellegrino, B. A. Habecker, and N. M. Nathanson carried out the cell transfection and functional studies. Drs. M. A. B. Melone, A. F. Hahn, H. Boman, M. Nolano, and N. M. Nathanson drafted the manuscript, which was circulated, amended, and approved by all authors.

Conflict of Interest

None declared.

References

1. Dagoneau N, Scheffer D, Huber C, et al. Null leukemia inhibitory factor receptor (*LIFR*) mutations in

Stüve-Wiedemann/Schwartz-Jampel type 2 syndrome. Am J Hum Genet 2004;74:298–305.
2. Hahn AF, Jones DL, Knappskog PM, et al. Cold-induced sweating syndrome. A report of two cases and demonstration of genetic heterogeneity. J Neurol Sci 2006;250:62–70.
3. Akawi NA, Ali BR, Al-Gazali L. Stüve-Wiedemann syndrome and related bent bone dysplasias. Clin Genet 2012;82:12–21.
4. Numata S, Hamada T, Teye K, et al. Complete maternal isodisomy of chromosome 5 in a Japanese patient with Netherton syndrome. J Invest Dermatol 2014;134:840–852.
5. Shahani BT, Halperin JJ, Boulu P, Cohen J. Sympathetic skin response- a method of assessing unmyelinated axon dysfunction in peripheral neuropathies. J Neurol Neurosurg Psychiatry 1984;47:536–542.
6. Fealey RD, Low PA, Thomas JE. Thermoregulatory sweating abnormalities in diabetes mellitus. Mayo Clin Proc 1989;64:617–628.
7. Provitera V, Nolano M, Caporaso BS, et al. Evaluation of sudomotor function in diabetes using the dynamic sweat test. Neurology 2010;74:50–56.
8. Nolano M, Provitera V, Perretti A, et al. Ross syndrome: a rare or misknown disorder of thermoregulation? A skin innervation study on 12 subjects. Brain 2006;129:2119–2131.
9. Nolano M, Provitera V, Crisci C, et al. Quantification of myelinated endings and mechanoreceptors in human digital skin. Ann Neurol 2003;54:197–205.
10. Purcell S, Neale B, Todd-Brown K, et al. PLINK: a tool set for whole-genome association and population-based linkage analysis. Am J Hum Genet 2007;81:559–575.
11. Haugarvoll K, Johansson S, Tzoulis C, et al. MRI characterization of adult onset alpha-methylacyl-coA racemase deficiency diagnosed by exome sequencing. Orphanet J Rare Dis 2013;8:1–11.
12. Li H, Durbin R. Fast and accurate short read alignment with Burrow-Wheeler transform. Bioinformatics 2009;25:1754–1760.
13. Crisponi G. Autosomal recessive disorder with muscle contractions resembling neonatal tetanus, characteristic face, camptodactyly, hyperthermia, and sudden death: a new syndrome. Am J Med Genet 1996;62:365–371.
14. Jung C, Dagoneau N, Baujat G, et al. Stüve-Wiedemann syndrome: long-term follow-up and genetic heterogeneity. Clin Genet 2010;77:266–272.
15. Knappskog PM, Majewski J, Livneh A, et al. Cold-induced sweating syndrome is caused by mutations in the *CRLF1* gene. Am J Hum Genet 2003;72:375–383.
16. Di Leo R, Nolano M, Boman H, et al. Central and peripheral autonomic failure in cold-induced sweating syndrome type 1. Neurology 2010;75:1567–1569.
17. Stanke M, Duong CV, Pape M, et al. Target-dependent specification of the neurotransmitter phenotype: cholinergic differentiation of sympathetic neurons is mediated in vivo by gp130 signaling. Development 2006;133:141–150.
18. Rousseau F, Gauchat J-F, McLeod JG, et al. Inactivation of cardiotrophin-like cytokine, a second ligand for CNTF receptor, leads to cold induced sweating syndrome in a patient. PNAS 2006;103:10068–10073.
19. Yeşil G, Lebre AS, Santos SD, et al. Stüve-Wiedemann syndrome: is it underrecognized? Am J Med Genet A 2014;164:2200–2205.
20. Kurth I, Pamminger T, Hennings JC, et al. Mutations in *FAM134B*, encoding a newly identified Golgi protein, cause severe sensory and autonomic neuropathy. Nat Genet 2009;41:1179–1181.
21. Sims NA, Johnson RW. Leukemia inhibitory factor: a paracrine mediator of bone metabolism. Growth Factors 2012;30:76–87.
22. Robinson WP. Mechanisms leading to uniparental disomy and their clinical consequences. Bioessays 2000;22:452–459.

Supporting Information

Additional Supporting Information may be found in the online version of this article:

Figure S1. DNA sequences of the region containing the LIFR c.2170C>G variant are illustrated. The father is normal (p.Pro724, CCC), whereas his daughter (patient) is homozygous (p.Pro724Ala, GCC) and the mother is heterozygous for the mutation.

Table S1. The table lists all unusual genetic findings on the patient´s chromosome 5. The list shows the ten variants with a frequency of less than 0.01 in the 1000Genomes database, plus the LIFR variant.

